in (Mn)-Cr.

The authors are grateful for the assistance of Mr. H. Oono for a part of experiments.

[1]G. De Vries, J. Phys. Radium 20, 438 (1959).

[2]Y. Hamaguchi, E. O. Wollan, and W. C. Koehler, Phys. Rev. 138, A737 (1965).

[3]S. Komura and H. Kunitomi, J. Phys. Soc. Japan 19, 103 (1965).

[4]H. B. Møller, A. L. Trego, and A. R. Mackintosh, Solid State Commun. 3, 137 (1965).

[5]T. Suzuki, J. Phys. Soc. Japan 21, 422 (1966).

[6]C. Koehler, R. M. Moon, A. L. Trego, and A. R. Mackintosh, Phys. Rev. 151, 414 (1966).

[7]Y. Ishikawa, S. Hoshino, and Y. Endoh, J. Phys. Soc. Japan 22, 1221 (1967).

[8]A. Arrott, S. A. Werner, and H. Kendrick, Phys. Rev. 153, 624 (1967).

[9]T. J. Bastow, Proc. Phys. Soc. (London) 88, 935 (1966).

[10]S. A. Werner, A. Arrott, and H. Kendrick, J. Appl. Phys. 38, 1243 (1967).

[11]Y. Endoh, Y. Ishikawa, and H. Ohno, Institute for Solid State Physics, University of Tokyo, Technical Report No. 266, 1967 (unpublished).

[12]Y. Ishikawa, Y. Endoh, H. Hashiura, and H. Ohno, Solid State Commun. 4, 657 (1966).

[13]S. Arajs and G. R. Dunmyre, J. Appl. Phys. 37, 1017 (1966).

[14]K. Schröder, M. J. Yessik, and N. P. Baum, J. Appl. Phys. 37, 1019 (1966).

[15]J. K. Tien and R. B. Gorden, Am. Soc. Mech. Eng., Paper 64 WA/PT-20 (1964).

TRANSMISSION SPIN RESONANCE OF COUPLED LOCAL-MOMENT AND CONDUCTION-ELECTRON SYSTEMS*

S. Schultz and M. R. Shanabarger†
University of California, San Diego, La Jolla, California

and

P. M. Platzman
Bell Telephone Laboratories, Murray Hill, New Jersey

(Received 10 August 1967)

Detailed measurements of the transmission spin resonance in dilute Cu-Mn and preliminary measurements in dilute Ag-Mn alloys have been made over the range 1.4-35°K. While many of the features of the conduction-electron–local-moment system are accounted for by an extended Hasegawa model, some significant anomalies remain. The first observation of conduction-electron spin resonance in pure silver is reported.

Recently there has been a great deal of interest in the properties of dilute magnetic moments in metals. Inasmuch as anomalies in this system are expected to depend on electron-impurity spin-flip cross sections and related properties,[1] it seems natural to expect that magnetic resonance experiments might provide direction information about the details of the system. Electron-spin-resonance measurements in the Cu-Mn system have been made by reflection[2,3] and transmission techniques.[4] We have measured the temperature and concentration dependence of the g values, linewidths, and line shapes of transmission signals in thin slabs of dilute Cu-Mn and Ag-Mn single-crystal alloys. We have been able to explain much of these data using a simple phenomenological theory similar to that proposed by Hasegawa[5] which has been extended to include the effects of electron diffusion, direct Mn relaxation, differences in the local-moment and conduction-electron g values, and the finite thickness of the sample. While the theory does account for most of the data, it is unable to predict certain striking anomalies. From linewidth data, where the theory does satisfactorily describe the experiments we have been able to determine the intrinsic Mn relaxation time to the lattice (T_{dl}), the spin susceptibility of the conduction electrons in copper (χ_s), and the spin-flip scattering rate of the conduction electrons in copper by the Mn impurities. It is possible that an accurate value for the effective s-d exchange coupling (J) may be determined from further analysis of the data, and at present we infer that J is negative and $0.1 < 0.4$ eV for Mn in Cu. We also report the first observation of the conduction-electron spin resonance (cesr) in pure silver with the g value 1.983 ± 0.001.[6]

The experimental technique is the same as that recently employed to discover cesr in several new metals.[7] Namely, a transmission experiment is performed in which microwave power is selectively transmitted through the metal sample when the cesr condition is satisfied. Since there are relatively few mechanisms for transmitting power through metal samples many times thicker than a skin depth, this technique allows one to make unambiguous identification of pure cesr and the related signals reported here.[8] The quantity which we measure is the component of the transmitted field projected onto a larger reference field at the same frequency. The samples were thinned to ≈0.003 cm from slices cut from single-crystal boules. The alloy crystals were grown under vacuum ($\cong 10^{-6}$ Torr) in carbon crucibles. The pure Cu and Ag used for alloying typically had resistivity ratios $\rho_{300°\mathrm{K}}/\rho_{4°\mathrm{K}}$ of $\cong$1000. Single crystals used for the g-value determinations of the pure metals have been specially treated resulting in resistivity ratios of 5000 to 15 000.

Theory.—The model we adopt to interpret the data is similar to that of Hasegawa.[5] The local moment and electron spins are cross relaxing with rates $1/T_{ds}$ and $1/T_{sd}$, respectively.[9] Both sets of spins can relax to the lattice with rates $1/T_{dl}$ and $1/T_{sl}$. The macroscopic magnetization in the specimen satisfies a pair of coupled, Bloch-like equations modified for exchange and diffusion:

$$\dot{\vec{M}}_s=\gamma_s[\vec{M}_s\times\vec{H}]+\gamma_s\lambda(\vec{M}_s\times\vec{M}_d)-(T_{sd})^{-1}\vec{M}_s+(T_{ds})^{-1}\vec{M}_d-(T_{sl})^{-1}(\vec{M}_s-\vec{M}_s{}^0)+D\nabla^2\vec{M}_s,$$
$$\dot{\vec{M}}_d=\gamma_d[\vec{M}_d\times\vec{H}]+\gamma_d\lambda(\vec{M}_d\times\vec{M}_s)+(T_{sd})^{-1}\vec{M}_s-(T_{ds})^{-1}\vec{M}_d-(\vec{M}_d-\vec{M}_d{}^0)/T_{dl}. \quad (1)$$

Here $\vec{M}_s$ and $\vec{M}_d$ are the magnetization vectors for the conduction electrons and local moments, respectively, and γ_s and γ_d are their gyromagnetic ratios. The parameter λ characterizes the strength of an effective field coupling the two systems. In a s-d exchange model λ is related to the exchange integral J by $\lambda=2J\Omega\hbar^2/\gamma_s\gamma_d$, where Ω is an appropriate atomic volume characterizing the range of the exchange interaction. The quantity D is the diffusion constant for the conduction electrons, $D=\frac{1}{3}V_{\mathrm{F}}{}^2\tau$, where τ is a phenomenological momentum collision time. The addition of the diffusion term to the Bloch equations correctly takes into account the motion of the electrons in cesr.[10]

Equations (1) provide a phenomenological description of the "electron bottleneck" phenomenon.[3] From equilibrium considerations, $T_{ds}/T_{sd}=\chi_d/\chi_s\equiv\chi_r$.[5] Equations (1) along with Maxwell's equations and an appropriate boundary condition on the magnetization at both faces of the slab provide a complete set of phenomenological equations which may be solved for the transmitted field.[11] Assuming that the sample thickness (L) is large compared with the microwave skin depth and $\chi\ll\lambda\chi\ll 1$, we find that the transmitted field may be expressed as[12]

$$H_T=(Q/K_2)\{1-\omega_d\chi_d\tilde{\lambda}/\Delta\}^2(\sinh K_2L)^{-1}. \quad (2)$$

Q is a constant which, for the range of concentrations considered, is essentially independent of the applied dc field, $\tilde{\lambda}\equiv\lambda+iW$ with $W^{-1}=T_{sd}\times\chi_d\omega_s$. $\Delta=\omega-\omega_d(1+\tilde{\lambda}\chi_s)+i/T_{dl}$ and

$$DK_2{}^2=2i\left(\omega-\omega_s-\frac{i}{T_{sl}}-\frac{\omega_s(\omega-\omega_d-i/T_{dl})\tilde{\lambda}\chi_d}{\Delta}\right). \quad (3)$$

When $\tilde{\lambda}=0$, i.e., no coupling between the spin systems, the solution given by Eqs. (2) and (3) reduces to the standard Dysonian transmission formula for a thick slab.[13] For any value of $\tilde{\lambda}$ the resonance is principally due to a near vanishing of K_2. In general there are two values of the magnetic field, corresponding to the two spin degrees of freedom, where K_2 has such a minimum. In practice one resonance mode is strongly damped, i.e., its width is of the order of $1/T_{ds}$, whereas the other root, the observed root, has a width which is of order $1/T_{sl}$.

The solution for the transmitted field given in Eqs. (2) and (3) is sufficiently complicated so that it is convenient to consider a limiting case which fits the principal features of the data. If the coupling is large, i.e., $|\omega_s-\omega_d|/\omega<|\tilde{\lambda}|\chi_s$ and $\omega_s\simeq\omega_d\simeq\omega$, Eqs. (2) and (3) reduce to

$$H_T=(Q/K_2)(1+\chi_r)^2(\sinh K_2L)^{-1}, \quad (4)$$

$$D^*K_2{}^2=2[1+i(\omega-\omega_m)T_{\mathrm{eff}}], \quad (5)$$

where

$$\omega_m = \omega_s + \frac{(\omega_d - \omega_s)\chi_r}{1+\chi_r}, \tag{6}$$

$$D^* = \frac{1}{3} V_F{}^2 \left(\frac{\tau}{1+\chi_r}\right), \tag{7}$$

and

$$\frac{1}{T_{\mathrm{eff}}} = \frac{(1/T_{sl})[1+(T_{sl}/T_{dl})\chi_r]}{1+\chi_r}. \tag{8}$$

Equations (4) and (5) are mathematically identical to the pure cesr transmission problem.[13]

Comparison with experiments.—The most striking feature of these observations is the variation of the position of the resonance maximum with temperature. These data are presented in Fig. 1. In the limit of strong exchange coupling, Eq. (5) would predict the measured g value (g_m) to be $g_m = g_s + (g_d - g_s)\chi_r/(1+\chi_r)$. Experimentally g_s is known for both copper and silver from the observed pure cesr and we take g_d to be the low-temperature g value as seen in reflection at higher concentrations.[14] The model predicts that at low temperatures there will be a line centered at the local-moment resonance which will shift as $(1+aT)^{-1}$, asymptotically reaching the pure cesr host g value at higher temperatures. Qualitatively, the data presented in Fig. 1 have the predicted behavior. However, the measured g values reach a plateau value quite far from that for the pure copper or silver resonance. For copper (including other data not presented in Fig. 1) we have found that at low concentrations the plateau is proportional to the local moment concentration (C_d). An attempt was made to fit the Cu-Mn data to an expression like Eq. (5) but with the assumption that the high-temperature g value of the host is C_d dependent. We find that the data cannot then be fitted to the observed g values in the low-temperature region where the measurements are most accurate. Indeed, using a value for χ_r as determined from the linewidth data (as discussed later), and reformulating Eq. (6) so as to allow g_p to appear as an intercept in a linear relation, invariably yields values very close to the g value for pure copper, and the slope yields values close to g_d. We are left with the conclusion that initially, and until temperatures close to where the plateau sets in,

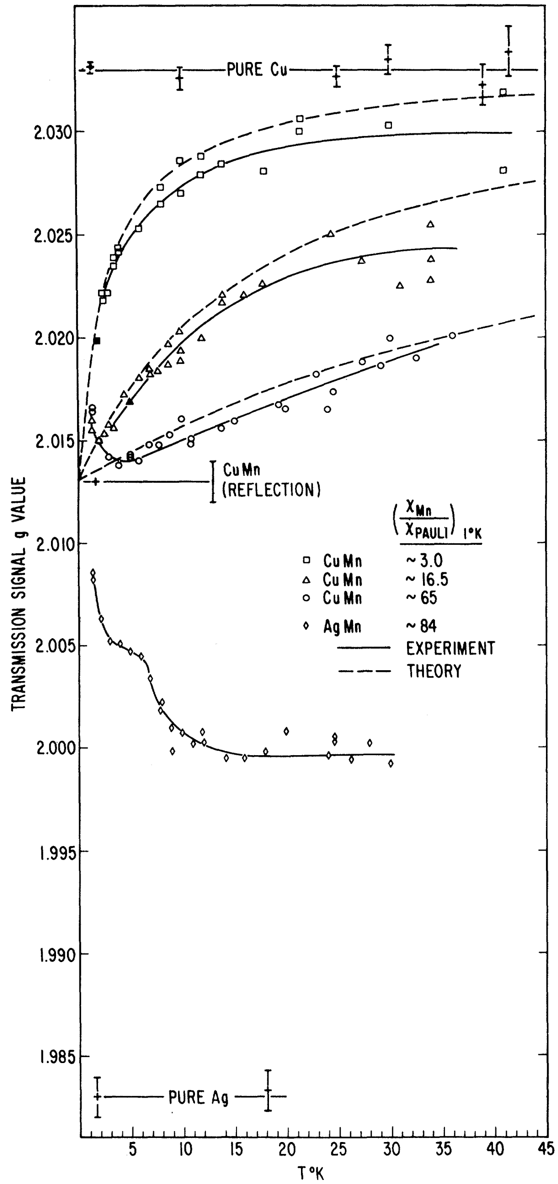

FIG. 1. Plot of the g value of the peak of the transmission resonance signals versus T for three CuMn samples and one Ag-Mn sample. The pure Cu and Ag g values as a function of temperature are also presented. The theoretical curves were obtained as explained in the text using $g_{\mathrm{Cu}} = 2.033$, $g_{\mathrm{Mn}} = 2.013$, and the susceptibility ratio as shown. A susceptibility ratio of 3 corresponds to ≈ 13 ppm of Mn in Cu. For Ag a ratio of 84 corresponds to ≈ 110 ppm of Mn. The approximate error in the data is indicated by the scatter of the points.

the g shifts do obey the relation predicted by the model.[15] This implies that near the plateau onset some other mechanism with a sharp temperature dependence becomes dominant.

A detailed fit of the linewidth data yields sev-

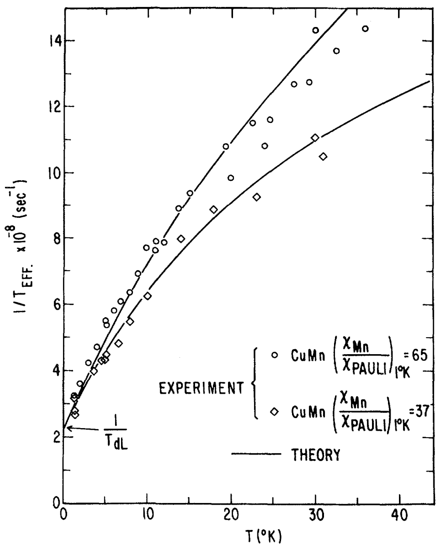

FIG. 2. Plot of $1/T_{\text{eff}}$ obtained from linewidth data versus the temperature. The theoretical curve is obtained from Eq. (8) using the values $1/T_{dl} = 2.56 \times 10^8\ \text{sec}^{-1}$, and $1/T_{sl} = 2.18 \times 10^9\ \text{sec}^{-1}$ and $4.0 \times 10^9\ \text{sec}^{-1}$ for the higher and lower concentration samples, respectively, and the susceptibility ratios as indicated on the figure. The error is $\simeq 5\%$ for $T < 20°\text{K}$ and $\sim 10\%$ for $T > 20°\text{K}$.

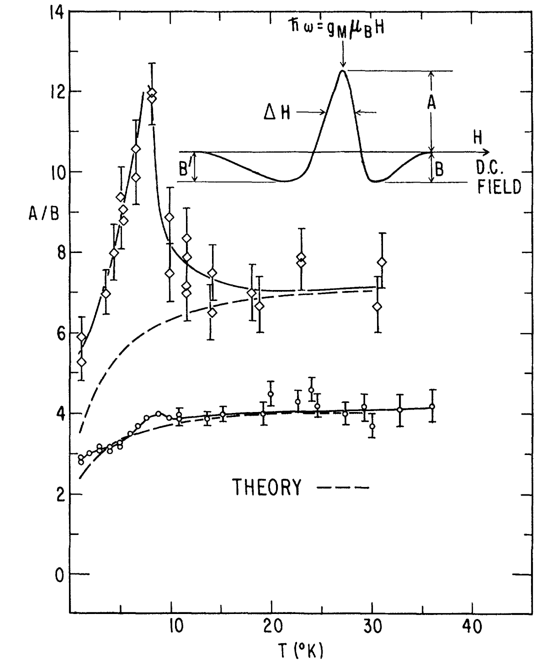

FIG. 3. Plot of A/B ratio versus the temperature for the same two samples as in Fig. 2. The insert represents a typical transmission signal as a function of magnetic field.

eral new experimental numbers. Within the framework of this model the observed linewidths can be converted into the relaxation time T_{eff} given in Eq. (8). In Fig. 2 we present typical data for $1/T_{\text{eff}}$ versus sample temperature for two values of C_d. The solid line is a theoretical fit to the data using parameters obtained as follows: The intercept at $T = 0°\text{K}$ yields $1/T_{dl}$. Once T_{dl} is known, one can reformulate Eq. (8) as a linear relation where the intercept at $T = 0°\text{K}$ now yields T_{sl}, and the slope yields χ_r at 1°K. For Mn in Cu we find $T_{dl} = (3.9 \pm 0.5) \times 10^{-9}$ sec independent of C_d. A preliminary value for Mn in Ag is $T_{dl} = 2.9 \times 10^{-9}$ sec.

Since the local-moment susceptibility of the sample can be directly measured or calculated from the known susceptibility/ppm and the "effective" C_d, we can use χ_r at 1°K to determine the electronic susceptibility χ_s of the host metal. Our current best value for $\chi_{\text{Cu}} = (1.6 \pm 0.4) \times 10^{-6}$. Since $\chi_r = T_{ds}/T_{sd}$ is proportional to the density of states[5] at the Fermi surface $n(\epsilon_{\text{F}})$, we find that $n(\epsilon_{\text{F}}) = 0.18 \pm 0.004\ \text{eV}^{-1}\ \text{atom}^{-1}\ \text{spin}^{-1}$. This is consistent within the error with the density of states determined from specific heat measurements.[16]

The quantity T_{sl}^{-1} when plotted against C_d is linear, with a finite intercept $(T_{sl}^0)^{-1}$ at zero. T_{sl}^0 is a measure of the spin-flip scattering rate for Cu electrons from the residual impurities in the "pure" material and is in good agreement with direct measurements ($T_{sl}^0 \cong 5 \times 10^{-9}$ sec). From the slope of the plot we find that the spin-flip scattering rate is $T_{sl} = (0.7 \pm 0.2) \times 10^{-11}$ sec (at.%).[17] The experimental uncertainty in T_{sl}, as is the case for χ_r, is mainly due to the uncertainty in the "effective" C_d.[18]

Cesr transmission line shapes are simply characterized by a location (g value), linewidth (ΔH), and peak to lobe (A/B) ratio (refer to insert in Fig. 3). In our current problem the resulting temperature behavior of the A/B ratio is quite different from the simple dependence found in cesr. In Fig. 3 we have presented the observed A/B ratio as a function of temperature for the same two Cu-Mn samples shown in Fig. 2. The solid line is the result of the theory, obtained from computer evaluations of Eqs. (4)-(8) using the parameters as determined from the linewidth data. The over-all behavior is qualitatively reasonable except for the resonancelike structure around 7°K. We have observed this behavior in other samples but have not been able to correlate this dramatic change with any of the other measured quantities, such as the relative signal intensity and dc resistivity. In fact, the observed relative intensity is in good agreement with the predictions of the model.

So far we have limited our discussion and comparison with the data to the limit of strong exchange coupling. In this limit the transmitted line shapes when adjusted to have equal lobes ($B=B'$) are symmetric about the peak value corresponding to the resonance condition. We actually find that when the lobes are made equal, there is a definite asymmetry in the line. Attempts to account for this asymmetry have been made by studying the nature of the solutions of Eqs. (2) and (3) for smaller values of J. For values of $J<|0.5|$ eV a definite asymmetry is predicted. From the sign of the asymmetry we are able to conclude that $J<0$. Preliminary attempts to fit the magnitude of the asymmetry lead us to conclude that $0.1<-J<0.4$. However, it may be necessary to have the explanation for the plateau g shift and the A/B anomaly before one will be able to decide definitely how far this model can be pushed to account for all the observed effects.

We feel that the spin transmission technique is a powerful new tool for studying the general problem of electrons interacting with dilute magnetic impurities. Although much of the data presented here seems to be quantitatively accounted for by a "simple" phenomenological model, there are still a number of important unresolved pieces of data. An understanding of these puzzles must ultimately rest on a detailed microscopic picture of the electron–local-moment (or moments) interaction.

We wish to thank Professor G. Goles and Professor M. Peterson for generously helping us with the concentration analysis, and Dr. A. Joseph for supplying us with a silver single crystal. We thank G. Dunifer for this help with the programming, and P. Monod for making resistivity measurements. We wish to thank Professor P. Pincus, Dr. Y. Yafet, and Dr. A. Gossard for helpful conversations.

---

*Work supported by the National Science Foundation.

†Submitted in partial fulfillment for the Ph.D. degree.

[1]J. Kondo, Progr. Theoret. Phys. (Kyoto) 32, 37 (1964); H. Suhl and D. Wong, Physics 3, 17 (1967).

[2]J. Owen, M. Browne, W. D. Knight, and C. Kittel, Phys. Rev. 102, 1501 (1956); J. Owen, M. Browne, V. Arp, and A. F. Kip, J. Phys. Chem. Solids 2, 85 (1957).

[3]A. C. Gossard, A. J. Heeger, and J. H. Wernick, J. Appl. Phys. 38, 1251 (1967).

[4]David L. Cowan, Phys. Rev. Letters 18, 770 (1967).

[5]H. Hasegawa, Progr. Theoret. Phys. (Kyoto) 21, 483 (1959).

[6]A spurious value for cesr in Ag has been reported by M. J. A. Smith, K. A. Hay, and D. C. Laine, Paramagnetic Resonance, edited by W. Low (Academic Press, Inc., New York, 1963), Vol. II, p. 785. A full report on the cesr in Ag will be forthcoming.

[7]S. Schultz, G. Dunifer, and C. Latham, Phys. Letters 23, 192 (1966), and references therein.

[8]Typically for the higher concentration samples where the "geometric cyclotron" leakage (Ref. 7) was very small, the power coming through the sample at resonance was 100 times greater than the off-resonance leakage power.

[9]The quantities T_{ds} and T_{sd} are defined in terms of the exchange integral J and are given explicitly in Ref. 5.

[10]Jerome I. Kaplan, Phys. Rev. 115, 575 (1959); G. D. Gaspari, Phys. Rev. 151, 215 (1966).

[11]The boundary condition on $\boldsymbol{M}_s$ is $\nabla\vec{M}_s=0$ at the surfaces. This corresponds to the condition that no magnetization leaves the sample and that there is no specific surface relaxation.

[12]We have solved the same equations for the reflected wave in a semi-infinite medium and although related effects to those reported here are in principle present in reflection, experimental difficulties preclude their being readily observed.

[13]M. Lampe and P. M. Platzman, Phys. Rev. 150, 340 (1966).

[14]g_d for CuMn was determined from a 500-ppm Mn sample in reflection after suitable corrections were made for line shape and demagnetization fields. g_d for Mn in Ag is not accurately known at present. As is evident from this work, care must be taken in assigning a "pure" g value in the event that impurities are present which give rise to temperature-independent g shifts. The constancy of our pure-Cu g value for several sources of supply and a wide range of resistivity ratio lead us to believe the value given is intrinsic. Preliminary measurements indicate no g shift when nonlocal-moment impurities are added. (P. Monod, private communication.) Estimates of possible residual g shifts indicate that this should be the case (Y. Yafet, private communication).

[15]For the higher concentration Cu-Mn samples at low temperatures we observe that the g shifts (relative to pure Cu) can actually go through a maximum. We believe the deviation from the model in this instance is due to the onset of ordering of the Mn. For the highest concentration Cu-Mn sample $[(\chi_{Mn}/\chi_{Pauli})_{1°K}=65]$ shown in Fig. 1, we have measured the resistivity as a function of temperature and find that the maximum g-shift coincides with the onset of deviation from the expected $\ln T$ dependence.

[16]T. Esterman, S. Friedberg, and J. Goldman, Phys. Rev. 87, 582 (1952). A precise comparison between the two values obtained for $n(\epsilon_F)$ involves a knowledge of the many-body corrections to χ_s. When the concen-

tration analysis is improved, such considerations will be warranted.

[17]This value is comparable with that obtained in Ref. 3.

[18]We have utilized residual resistivity, neutron activation, and optical absorption to aid in the C_d analysis. Care has been exercised to reduce the possibility of Mn oxidation. D. H. Howling, Phys. Rev. 155, 642 (1967). However, the most serious current experimental problem is the determination of the "effective" Mn concentration in the low-ppm range.

EXPERIMENTAL STUDY OF THE ($He^3, d\tilde{p}$) REACTION*

R. A. Hoffswell, D. Jamnik, T. M. Noweir, and A. I. Yavin
Department of Physics, University of Illinois, Urbana, Illinois
(Received 14 August 1967)

The (He^3, d) stripping reaction, which is similar to the (d,n) reaction, is now extensively used because of the advantage in observing an outgoing charged particle. The (He^3, d) reaction at medium energy is known to be direct and to strongly excite isobaric analog states. These states, when proton-unstable, have recently been investigated by the observation of their decay protons.[1] This method has also been used for the study of the (d,n) reaction.[2] It is natural to expect that the advantages of the (He^3, d) reaction and the proton-decay method can be combined in studying the following sequential reaction:

$$Z^A + \mathrm{He}^3 \to (Z+1)^{A+1} + d; \quad (Z+1)^{A+1} \to Z^A + \tilde{p},$$

where the notation $\tilde{p}$ emphasizes the fact that the proton results from the decay of the intermediate-product nucleus. Information on the excitation of the intermediate nucleus $(Z+1)^{A+1}$ is gotten in the usual way by observing the deuteron spectrum, while decay properties of the intermediate states, as well as properties of states of the final nucleus, can be studied by observing the spectrum of coincidences between the deuterons and the decay protons. We present here the results of an experimental study of such a sequential reaction on Zr^{90}. Data based on brief ($He^3, d\tilde{p}$) experiments on Zr^{91} and Zr^{92}, as well as C^{12} and O^{16}, will also be discussed.

The zirconium targets were self-supported and isotopically enriched, while Mylar was used for the study of C^{12} and O^{16}. An 18.7-MeV He^3 beam was used in the experiments, with beam currents limited to about 40 nA to prevent excessive counting rates due to elastic scattering. 55- and 1000-μ silicon detectors were used in two E-ΔE mass-discrimination systems for the detection of coincident protons and deuterons. The proton telescope included a third detector to discriminate against transmitted particles. Both systems were adjusted to have identical gain. The data were displayed on a 64×64-channel analyzer with a channel width of 182 keV. The energy stability was better than ±0.5 % per day. Scattering angles were selected at 90° and 270° for protons and deuterons, respectively, and each solid angle was 5.5×10^{-3} sr. Observed counting rates were 60 counts per hour, with accidentals accounting for less than 5 % of the total counts. The $Zr^{90}(He^3, d\tilde{p})Zr^{90}$ data were accumulated for 33 h. Channels were sometimes added in order to get statistically meaningful results.

The energy dependence of the Nb^{91} excitation in the one-step reaction $Zr^{90}(He^3, d)Nb^{91}$ is shown in Fig. 1(a). A similar structure is seen in Fig. 1(b), which displays deuterons in coincidence with decay protons and is free from contribution from C^{12} and O^{16} contaminants. The cutoff at the lower energy side of Fig. 1(b) is apparently due to the opening of neutron channels, while the cutoff at the higher energy side is due to the coincidence requirement on the protons. The cutoff at the neutron threshold suggests that the direct break-up of He^3 into a deuteron and a proton is very small and that the proton width is much smaller than the neutron width above the neutron threshold, in agreement with a recent ($p, n\tilde{p}$) study.[3] Similar conclusions are derived from the observed small magnitude of the ($He^3, d\tilde{p}$) cross section for Zr^{91} and Zr^{92}, for which the isobaric analog states (IAS) of the ground states are already neutron-unstable.

The prominent (starred) peaks of Fig. 1 correspond to the excitation in Nb^{91} of the ground IAS of Zr^{91}, while the structure at lower channels corresponds to excitation of excited IAS.